10 January 2002

ELSEVIER

Chemical Physics Letters 351 (2002) 213–221

CHEMICAL PHYSICS LETTERS

www.elsevier.com/locate/cplett

Photon echo pulse sequences with femtosecond shaped laser pulses as a vehicle for molecule-based quantum computation

Vadim V. Lozovoy, Marcos Dantus *

Department of Chemistry and Department of Physics, Michigan State University, East Lansing, MI 48824-1322, USA

Received 23 May 2001; in final form 22 August 2001

Abstract

We propose three-pulse four-wave mixing (FWM) in cooled molecules for computation. Femtosecond amplitude and phase shaped pulses encode information into a coherent superposition of vibrational states. The coherent coupling between the quantum states and the consecutive interactions with shaped pulses is used as quantum logic gates to create the final superposition of states. The resulting coherent virtual or stimulated photon echo signal corresponds to a vector or a matrix output, respectively. Photon echo is the optical analog to spin echo where inhomogeneous decoherence is cancelled. The experimental setup required is discussed and preliminary results are presented. © 2002 Published by Elsevier Science B.V.

1. Introduction

During the past decade, interest in the subject of quantum information technology (QIT) has grown exponentially. For current reviews of the field the reader is referred to a number of excellent books and review articles [1–4], here we concentrate on the essentials. The main difference between QIT and its classical cousin, IT, is the phase coherence of quantum systems. Coherence opens the possibility of following many computational paths simultaneously, and achieving massive parallelism. The power of quantum computing derives from the interference inherent among the various quantum paths the system can take from a prepared input to an output that can be read out [5]. The quantum computer can therefore solve certain problems that could not be practically solved by conventional computers [6,7]. The main requirement for a quantum computer is a quantum set of states that can be addressed coherently and controlled by matrix transformations without the loss of coherence. Possible candidates that have been demonstrated experimentally include ion traps [8], cavity quantum electrodynamics [9], magnetic resonance [10] and Rydberg wave packets [11]. Here we propose to use three-pulse four-wave mixing (FWM), in particular the photon echo and virtual echo (VE) pulse sequences, to prepare, control and interrogate coherent ensembles of vibrational states [12]. The transformations are achieved with femtosecond amplitude and phase shaped laser pulses in a timescale that is short compared to decoherence. The output corresponds

* Corresponding author. Fax: +1-517-353-1793.
E-mail address: dantus@msu.edu (M. Dantus).

0009-2614/02/$ - see front matter
PII: S0009-2614(01)01388-4

to the coherent FWM emission. The theoretical foundation for these experiments is based on the third-order density matrix [13].

The proposed experiments involve the coherent manipulation of vibrational states in molecular iodine using FWM [12,14–18]. Zadoyan et al. [19] recently considered the manipulation of ro-vibronic superpositions using time-frequency-resolved coherent anti-Stokes Raman scattering (TFRCARS) for quantum computing. In Zadoyan's experiment, the evolution of the rovibrational states is proposed to carry out the computation. The difficulties with using only the intramolecular dynamics of a quantum oscillator for computation have been described in [4]. The work proposed here differs from Zadoyan's in that pulses carrying phase and amplitude information achieve the specific transformations. This gives our method the power to carry out complex operations. Our previous work [14] shows that the use of interference between Liouville pathways as proposed in [19] for making a two qubit controlled gate would be complicated by waved packet spreading [15]. Our approach does not depend on wave packet dynamics of the system because the amplitude and phase shaped pulses control the transition probabilities between rovibrational ground and excited states in the frequency domain.

A number of different methods can be conceived, based on three-pulse FWM, to demonstrate molecule-based computation. The main idea behind the proposed QIT is to write and store information as quantum amplitudes on selected eigenstates (see Fig. 1a) and to manipulate the information with shaped coherent light pulses (see Fig. 1b). The shaped pulse contains specific spectral components that address directly v'–v'' transi-

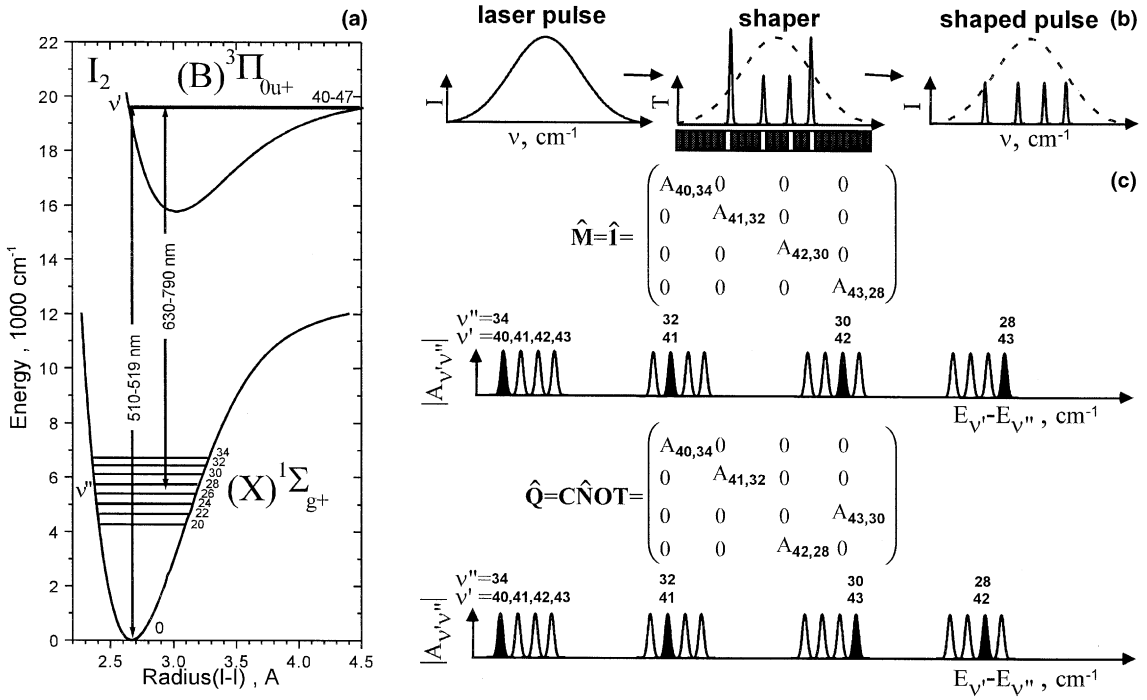

Fig. 1. (a) Energy curves, vibrational levels for ground and first excited states of the iodine molecule and spectral ranges of optical transitions for a 3-qubit processor. (b) The initial transform limited femtosecond laser pulse passes through a shaper and is transformed into coherent light consisting of several narrow spectral components. The frequency components are determined by the spatial light modulator. (c) Electric field components for the transitions from excited to ground states are responsible for the unit matrix **M** and controlled not quantum gate **CNOT** for the 2-qubit operators (see text). Additional amplitude and phase corrections of the Franck–Condon factors and anharmonic vibrational dynamics are also performed by the shaper for each separate spectral component.

tions. For example, in Fig. 1b we illustrate the transformation from four vibrational states $(40, 41, 42, 43)$ in the B state to a set of four vibrational states $(34, 32, 30, 28)$ in the X state. In the first case (operation called M – writing in memory) we promote the transitions $40 \rightarrow 34$, $41 \rightarrow 32$, $42 \rightarrow 30$, $43 \rightarrow 28$. These components are shown in black (Fig. 1c). To promote a different transition, for example, to construct quantum gate CNOT (operator Q), we must use different spectral components for the transitions $40 \rightarrow 34$, $41 \rightarrow 32$, $42 \rightarrow 28$, $43 \rightarrow 30$. Each specific vibrational eigenstate is a component of a vector in Hilbert space and the manipulation with complex amplitudes of these vector components allows us to perform quantum computations.

Here we present two different arrangements that provide the foundation of a more general setup for vectorial computation. The FWM response in molecular iodine a quasi-two level system can be calculated using the density matrix formalism and can be summarized using four Liouville pathways known as R_1, R_2, R_3 and R_4 (see Fig. 2a,b) [13]. The pathways are presented as ladder diagrams. The two horizontal lines represent the ground and excited states. Time evolves from left to right. Signal due to R_2 and R_3 is known as photon echo or stimulated photon echo, whereas signal from R_1 and R_4 is known as VE [12,15]. The implementation of the proposed experiments takes advantage of the well-known Franck–Condon factors for molecular iodine [20]. The first pump pulse spans the wavelength range 510–519 nm (Fig. 1a), where the absorption cross-section from the ground state is maximal. The second Stokes pulse is tuned to a wavelength where no further B state excitation can be achieved from the ground state $(v'' = 0)$. In the wavelength range 630–790 nm (Fig. 1a), the Stokes pulse is optimized to stimulate transitions to the ground state. The choice of wavelengths is similar to the TFRCARS setup [19]. This combination (Fig. 2a,b) of laser wavelengths minimizes the contribution of R_1 and R_2, but it optimizes the contributions of R_3 and R_4. These two responses are separated by their different phase matching conditions [12–15]. For R_4 experiments the probe pulse has the same wavelength as the Stokes pulse, while for R_3, the probe pulse has the same wave-

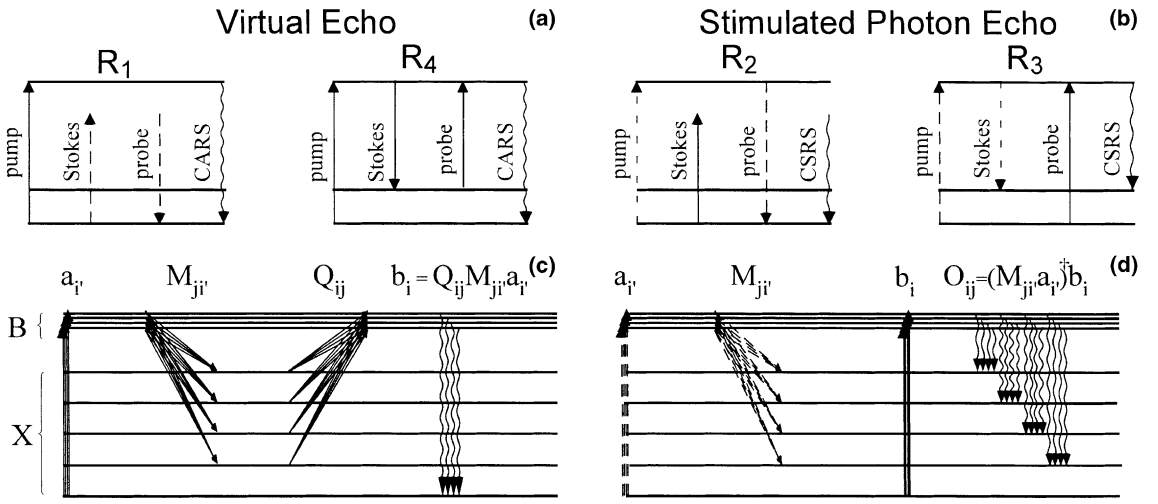

Fig. 2. Ladder diagrams for the proposed experiments. Horizontal lines represent energy levels. Arrows represent optical transitions between the ground and excited electronic states. Dashed arrows indicate *bra* interactions, solid arrows indicate *ket* interactions. Wavy arrows represent three-pulse stimulated FWM emission. Time in the diagrams goes from left to right. In all diagrams Stokes pulses are red shifted relative to the first pulse. For iodine, there are no resonance transitions from the initial state with the Stokes pulse. The Liouville pathways R_1 (a) and R_2 (b) are small because of this condition. (c) The VE signal has spectral components from transitions from the final excited states to the initial ground state. (d) The SPE signal has spectral components from transitions from the final excited states to the vibrational states in ground states.

length as the pump pulse. Work in our group has focused on demonstrating coherent control over superpositions of vibrational states in the ground and the excited ($B^3\Pi_{o+u}$) electronic state [12–15]. The signal detected in the phase-matching geometry for non-collinear pulses depends only on the third-order density matrix. Only signal resulting from the coherent interaction of the three laser beams with the molecules is detected. The shaped pulses, therefore, control the coherent transformation of each order of the density matrix.

2. Theory

Each of the laser three laser pulses interacts with the molecular ensemble and controls by quantum interference the evolution of the density matrix. For all cases, the first shaped pump pulse creates a coherent superposition of vibrational states in the excited state. Assuming weak interactions, we use first order perturbation theory for the analysis and say that each interaction increases the order of the wavefunctions state by one. The complex amplitude $a_{i'}$ of each excited vibrational state is defined by the spectrum of the electric field

$$|\Psi^{(1)}\rangle \propto \sum_{i'} a_{i'}|i'\rangle. \tag{1}$$

The second pulse (Stokes) promotes transitions (defined by the matrix elements M) to the coherent superposition of vibrational states in the ground electronic state (Liouville pathways R_4 and R_3)

$$|\Psi^{(2)}(\tau_{12})\rangle \propto \sum_{ji'} M_{ji'}a_{i'}|j\rangle. \tag{2}$$

Liouville pathways R_1 and R_2 have minimal contributions to the signal because they involve absorption from the ground state, which for the Stokes pulse wavelength is very small. If the wavelengths in the probe pulse are equal to those in the Stokes pulse, then the probe pulse promotes transitions (defined by matrix elements Q) from the ground state to the exited state (Liouville pathway R_4)

$$|\Psi^{(3)}(\tau_{12},\tau_{23})\rangle \propto \sum_{iji'} Q_{ij}M_{ji'}a_{i'}|i\rangle. \tag{3}$$

If the wavelengths in the probe pulse are equal to those in the pump pulse, then the probe pulse promotes transitions from the initial ground state to the excited state (Liouville pathway R_3)

$$|\Psi^{(1)}(\tau_{13})\rangle \propto \sum_{i} b_i|i\rangle. \tag{4}$$

The VE signal due to R_4 is formed by the coherence between the initial ground state and the third-order wave packet in the excited state. This emission has a phase matching direction $\mathbf{k}_3 - \mathbf{k}_2 + \mathbf{k}_1$ and a third-order polarization given by

$$P^{(\mathrm{VE})} \propto \langle \Psi^{(0)}|\mu|\Psi^{(3)}(\tau_{12},\tau_{13})\rangle. \tag{5}$$

Stimulated photon echo (SPE) signal due to R_3 is formed by the coherence between the second order wave packet in the ground state and the first order wave packet in the excited state. This emission has a phase matching direction $\mathbf{k}_3 + \mathbf{k}_2 - \mathbf{k}_1$ and a third-order polarization given by

$$P^{(\mathrm{SPE})} \propto \langle \Psi^{(2)}(\tau_{12})|\mu|\Psi^{(1)}(\tau_{13})\rangle. \tag{6}$$

The emitted light resulting from the third-order polarization is the output. This output may be measured or, after coherent amplification, used as input for a new quantum gate to make a circuit. In Fig. 3 we show the density matrix representation for the non-linear optical processes which take place for a model 5 level system, where 0 is the initial ground state, and g, g′ and e, e′ are vibrational states in the ground and excited states, respectively. Shaped external fields promote the density matrix transformations. The third-order polarization is the trace of the product of the dipole moment and the third-order density matrix [13]. From a mathematical point of view (see Fig. 3) the VE signal is a vector with components $b_i = \sum_{ji'} Q_{ij}M_{ji'}a_{i'}$ and the photon echo signal is a matrix $O_{ij} = (\sum_{i'} M_{ji'}a_{i'})^{\dagger}b_i$ (where † indicates the Hermitian conjugate).

3. Experiment and preliminary results

A regeneratively amplified Ti:Sapphire femtosecond laser system is used to produce ~ 45 fs pulses centered at 800 nm. Ultrafast (5–20 fs) pulses in the visible range are generated using

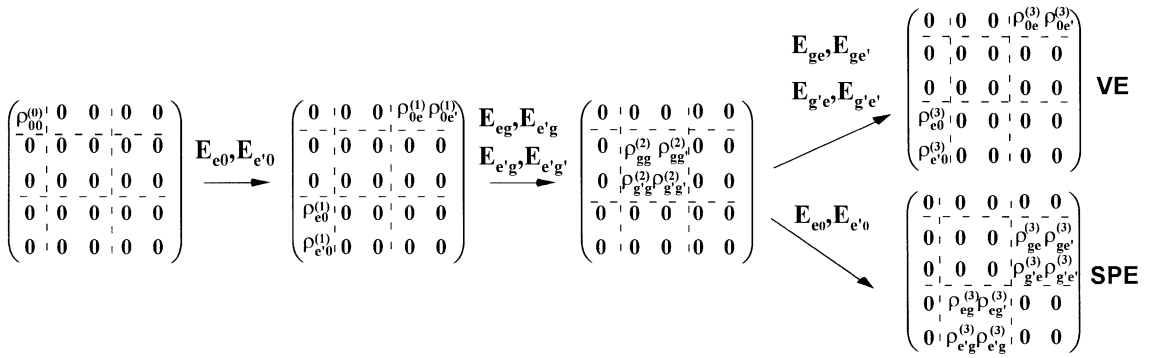

Fig. 3. The evolution of a 5×5 density matrix (DM) in external fields for the R_3 and R_4 Liouville pathways. The electric field components (above the arrows) are responsible for the optical transitions. Initially the system is represented by the zeroth-order non-coherent DM $\rho^{(0)}$. After the first pulse, the first order DM $\rho^{(1)}$ is generated, which is described by an electronic coherence between the ground and the excited state. After the second pulse, the second order DM $\rho^{(2)}$ can be described by the vibrational coherence in the ground state. The third pulse gives rise to the third-order DM $\rho^{(3)}$ that can be separated into two components, VE $\rho^{(\mathrm{VE})}$ (vibronical coherence between excited state and initial state) and SPE $\rho^{(\mathrm{SPE})}$ (represented by coherence between vibrational states in the excited state and vibrational states in the ground state). The VE and SPE spectral components of emission can represent a vector or a matrix, respectively.

non-collinear optical parametric amplifiers (NOPA) [21,22]. The femtosecond pulses are shaped in phase and amplitude using 128 (or more) element spatial light modulators [23]. Shaped pulses have been successfully used for the manipulation of Rydberg wave packets in atomic [24] and molecular dynamics [25,26]. The signal is dispersed in a spectrometer with a CCD to achieve spectral resolution. Ideally, the information carried by the coherent FWM output is heterodyne (phase sensitive) detected. The experimental implementation is shown as a schematic in Fig. 4a,b. The full implementation requires two NOPAs and three pulse-shapers. Here we present data obtained from molecular I_2 at ~ 90 °C. We include data using degenerate transform limited pulses at 620 nm to illustrate the VE and SPE signals [14]. We also include data involving the VE arrangement using a 595 nm pump, shaped 800 nm Stokes pulse and 800 nm probe pulse. Here we have used homodyne detection to demonstrate the feasibility of the experiments.

The experimental data presented in Fig. 4c correspond to the VE setup. Because the three beams are the same wavelength (620 nm), the timing of the first two pulses is used to determine which Liouville pathway leads to signal formation [12]. The data obtained for $\tau_{12} = 614$ fs results from the R_4 non-linear optical response. The signal shows the time evolution of the ground state coherence prepared after the first two pulses. The third pulse reads this coherence by transferring it to the excited state where the emission arises.

The data presented in Fig. 4d correspond to the SPE setup. Here the time delay between the first and last pulses, $\tau_{13} = 460$ fs, is set to cancel the contributions from the R_2 response so that the data result only from the R_3 non-linear optical response [12]. It is clear that every 307 fs, which is the period of oscillation of the wave packet in the excited state, in the signal achieves a maximum value. All laser pulses have their phases set to zero, so no specific quantum information has been introduced in the phase yet. Here we show the coherent manipulations of ground and excited state wave packets and the control over the desired responses R_3 and R_4.

The experimental data shown in Fig. 5 were obtained with a pump beam at 585 nm; a shaped Stokes beam centered at 800 nm and a probe beam at 800 nm. The phase-matched signal emerged centered near 590 nm and is clearly modulated by the rotationally broadened vibronic transitions. Although the sample was held near 463 K, the individual transitions can already be discerned. Jet cooling, however, will sharpen considerably the

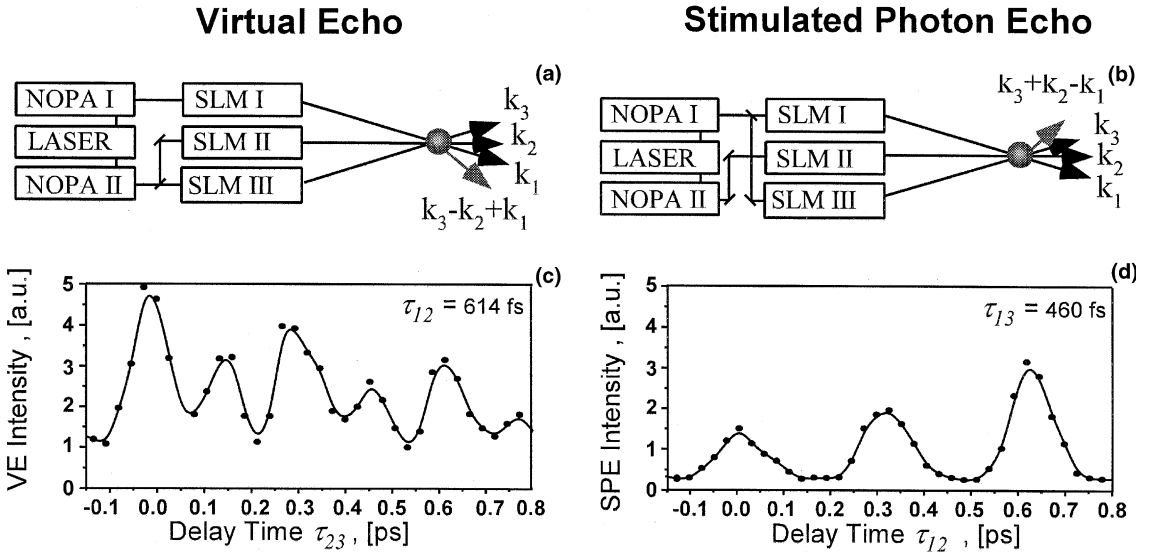

Fig. 4. Experimental setup for (a) VE and for (b) SPE types of computing. The NOPAs are pumped by a femtosecond Ti:sapphire amplified laser. Shaped pulses are formed by spatial light modulators. VE and SPE have wave vectors $\mathbf{k}_3 - \mathbf{k}_2 + \mathbf{k}_1$ and $\mathbf{k}_3 + \mathbf{k}_2 - \mathbf{k}_1$, respectively, and are homodyne or heterodyne detected. The homodyne detected intensities of VE (c) SPE (d) as function of time delay time between the pulses are presented. The VE signal shows the period of the ground state vibrations (160 fs). The R_4 process gives the major contribution to the VE signal. The SPE signal is maximum for delay times that correspond to vibrations in the excited state (310 fs). The R_3 process gives the major contribution to the SPE signal.

spectral resolution. Three different conditions are shown; in all cases the time delay between the first two pulses was fixed at 1 ps. Fig. 5b,c show the output when the second and third pulses are overlapped in time. Comparing these two results, we appreciate the effect of shaping the Stokes spectral amplitude (see Fig. 5a) on the output spectra. In Fig. 5d, the third pulse is delayed by 2.2 ps illustrating the influence of intramolecular dynamics.

4. Discussion

In order to address individual vibrational eigenstates, the spectral resolution needs to be $\sim 10\ \mathrm{cm}^{-1}$, based on a vibrational spacing of 40–50 cm^{-1} in the excited state [27]. Based on these parameters the time delay between pulses should be longer than 5 ps to prevent pulse overlap. The rotational constants for iodine are $B_X(v'' = 0) = 0.0373$ and $B_B(v' = 40\text{–}50) = 0.019\text{–}0.017$ [27]. The rotational Boltzmann distribution and dispersion of rotational distribution Δ_J is on the order of $\sqrt{k_B T_J/(2B_X hc)}$, where T_J is the rotational temperature. The spectral width of the rotational band $(B_X\text{–}B_B)\Delta J^2$ must be less than the spectral resolution 10 cm^{-1}. To achieve this condition the molecules must therefore be colder than 50 K. This will be achieved using a supersonic jet expansion.

The proposed quantum computer is based on the interference inherent among the various quantum paths the system can take given a specific input (three shaped pulses) to an output (the FWM coherent emission) that can be read out [5]. Regarding the scalability of the proposed method, the main parameter for quantum computation is the dimensionality (N) of the available Hilbert space. We can measure N as 2^n where n is number of qubits [1–4]. Our preliminary experiments involve $N = 2^2 = 4$ vibrational states. We estimate that we can easily achieve $N = 2^3 = 8$ or a 3-qubit machine (as shown in Fig. 1a). In Fig. 2 we illustrate 2-qubit operations. Using only vibrational states of molecular iodine it is possible to make a processor with $N = 2^5 = 32$. The combination of rotational states (as proposed in [19]) and con-

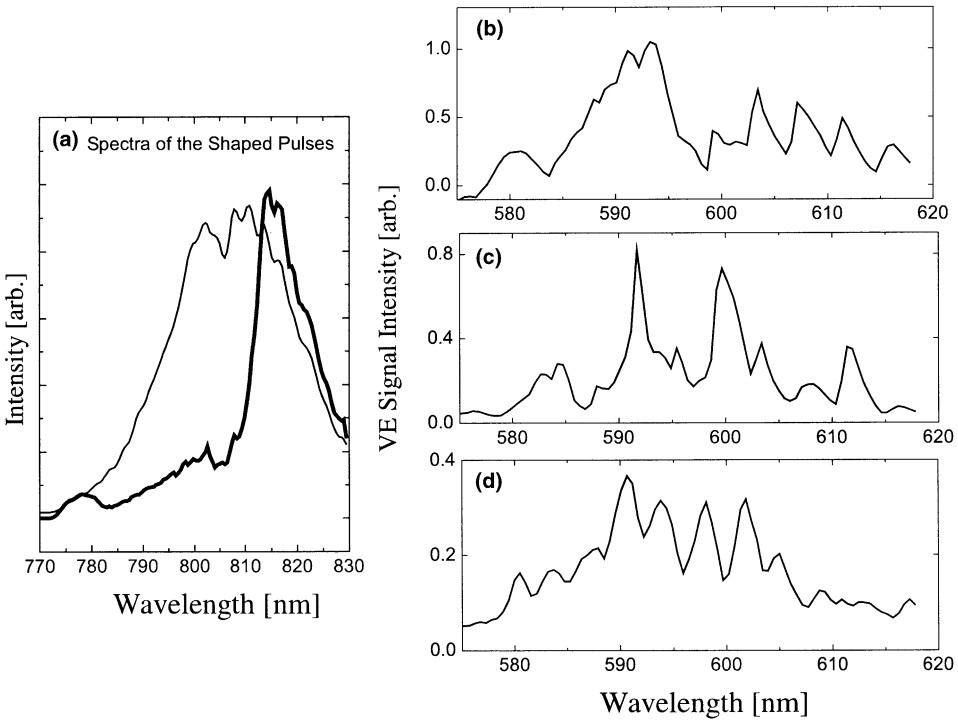

Fig. 5. Experimental data obtained with a 585 nm pump, 800 nm (shaped) Stokes and 800 nm probe pulses. (a) Spectra of the two Stokes pulses used in our experiments. The VE data shown in figures (b), (c), and (d) was obtained with a time delay between the first pulses fixed at 1 ps. For (b) and (c), the second and third pulses were overlapped in time. (b) Spectrum of the signal obtained with the pulses shaped as indicated by the thick line in (a). (c) Spectrum of the signal obtained with the pulses shaped as indicated by the thin line in (a). (d) Spectrum of the signal obtained as in (c) but after the third pulse was delayed by 2.2 ps.

trolled vibrations (as we propose in this article) could achieve a much greater Hilbert space, perhaps one with $N = 2^{10} = 1024$. If we only control amplitude and not phase, the number of independent colors that need to be controlled to load a binary number into an N-state register grows linearly with N. From this point of view, the scaling of the proposed method requires exponential resources, and would not be amenable to perform Shor's factorization algorithm [7]. Our method is based on interference and can be used to carry out computational tasks such as Grover type algorithms [5,35]. The efficiency of our method arises from the massive controlled interferences brought about by the three shaped laser pulses. The number of interfering pathways is quadratic on the number of available quantum eigenstates.

The first pulse serves to load the information (amplitude and phase) into the eigenstates to form vector a. The second pulse transfers the information into a temporary memory. This step can be a one-to-one transfer (unity matrix) or it can involve interference among different quantum pathways (matrix $\mathbf{M}$). The third pulse can play two different roles. In the PE setup, the third pulse loads new information (vector b) and the signal corresponds to the direct product, $a \otimes b$. This setup may be useful for information encryption carried out with two unknown sources. In the VE setup, the third pulse (matrix $\mathbf{Q}$) transforms vector a into a new vector by the product $\mathbf{Q}a$. The latter can perform complex computational tasks in one step, contrary to the methods based on binary quantum logic.

The number of participating molecules, photons, and the efficiency of the excitation and detection may give the quantum limit of the size of the molecular device based upon this proposed experiment. It is important to guard against an

exponential increase in physical resources in scaling up the implementation [28]. Better addressing schemes may be implemented to save on resources. So far, no experimental method has promised the scalability required for factoring a 500-digit number [29].

The output of a VE pulse sequence can be used as the input for a subsequent computation. For the SPE pulse sequence the output has the same spectral components as the quantum gates. These properties open the possibility to make complex networks. The experimental implementation would be complicated by the required amplification of the signal and the interaction with new pulses. Amplification noise should not be a problem, because the output is the coherent emission from a massive ensemble of identical molecules. Similar to NMR free induction, the photon echo does not destroy the information contained in the ensemble.

The last important issue we must discuss is decoherence. Our decoherence measurements [15] show that relaxation times for this system are in the hundreds of picoseconds timescale even at 470 K. With supersonic jet cooling, the relaxation time increases up to the sub-microsecond timescale. We showed earlier that the main source of decoherence is inhomogeneous broadening [15]. Taking advantage of this property has been considered [30]. After canceling homogeneous and inhomogeneous decoherence the main source of decay is spontaneous emission, which occurs for molecular iodine on the microsecond scale. Furthermore, if the information is stored in the ground electronic state, as proposed, then spontaneous emission is negligibly slow. The ratio between the time for quantum computation (10^{-11} s) and coherence lifetime (10^{-7} s) is approximately 10^4. This favorable ratio will permit complex operations with minimal loss of coherence.

5. Conclusion

The structured optical pulses for this molecule-based FWM computer can be treated as reset, write, and process operations and the time gated spectroscopic data can read out the result. The individual operations run at $a < 5$ ps clock speed, optical pulse shaping directly programs the phase and amplitude of the molecular wave packets. This molecular system may provide a massive number of operations in a large volume of the Hilbert space. The proposed method has some analogies to NMR-based quantum computation [4,31]. As pointed out by Warren [32], the NMR quantum computer has two problems. The first is low clock frequency, approximately 10–100 Hz. In our case, using optical frequencies, the clock rates are on the order of 10^{11}–10^{12} Hz. The second is that NMR operates in the high temperature limit. The NMR ratio of photon energy to the temperature is $h\nu/k_BT < 10^{-6}$ for a 10 spin system. If the system is sufficiently noisy, exponential resources are needed even if entanglement is present [33]. Clearly, entanglement, especially mixed state entanglement, should be better understood [34]. Certain quantum computation algorithms with polynomial speedup do not require entanglement [35]. Echo sequences, as proposed here, operate in the low temperature limit $h\nu/k_BT > 10^3$, operate on a 10^{11} Hz clock, and are thus immune to quantum noise and inhomogeneous decoherence. An additional advantage for non-linear optical methods is phase matching which allows us to manipulate the Liouville pathways separately or to combine them to achieve additional interferences.

From a mathematical point of view, the proposed VE and SPE processes can perform the following functions: write, store in memory, read, sum, scalar product, direct products, matrix product between matrices and vectors, and can be used to construct circuits and networks. We can use a method similar to that proposed by Bucksbaum and co-workers [11,24] for interference between two or more coherent wavefunctions to encrypt information or for mathematical summation. The large Hilbert space and the freedom to construct complex quantum gates give us the possibility to operate with massive coherent quantum information even within one three-pulse sequence. The drastic speed increase and greater resilience to noise over NMR are attractions of this approach. Quantum error correction, to protect against the effects of spurious environmental interactions as proposed by Shor [7], will not be

needed. Therefore, the implementation is much simpler and allows one-pass operations that do not require feedback. Work is proceeding in our laboratory on the full experimental implementation of the proposed method. The method is not restricted to gas phase iodine, quantum dots or other molecules in gas or condensed phases may have certain advantages.

Acknowledgements

This research was funded by the Chemical Sciences, Geosciences and Biosciences Division, Office of Basic Energy Sciences, Office of Science, U.S. Department of Energy and the National Science Foundation (CHE-9812584). Marcos Dantus is a Lucille and David Packard Science and Engineering Fellow. We are very thankful to Matthew Comstock and Igor Pastirk who implemented the setup and obtained the preliminary data presented here in record time. Without these data, the article would have been only a theoretical proposition.

References

[1] A. Steane, Rep. Prog. Phys. 61 (1998) 117.
[2] C.P. Williams, S.H. Clearwater, Exploration in Quantum Computing, Springer, New York, 1998.
[3] H.-K. Lo, S. Popescu, T. Spiller (Eds.), Introduction to Quantum Computation and Information, World Scientific, Singapore, 1998.
[4] M.A. Nielsen, I.L. Chuang, Quantum Computation and Quantum Information, Cambridge University Press, Cambridge, 2000.
[5] P. Knight, Science 287 (2000) 441.
[6] R. Feynman, Int. J. Theor. Phys. 21 (1982) 467.
[7] P. Shor, in: Proceedings of the 35th Annual Symposium on Foundation of Computer Science, 1994, p. 124.
[8] J.I. Cirac, P. Zoller, Phys. Rev. Lett. 74 (1995) 4091.
[9] Q.A. Turchette, C.J. Hood, W. Lange, H. Mabuchi, H.J. Kimble, Phys. Rev. Lett. 75 (1995) 4710.
[10] D. Cory, A. Fahmy, T. Havel, in: Proceedings of the 4th Workshop for Quantum Computation, Boston University, New England Complex System Institute, 1996, p. 87.
[11] J. Ahn, T.C. Weinacht, P.H. Bucksbaum, Science 287 (2000) 463.
[12] V.V. Lozovoy, B.I. Grimberg, I. Pastirk, M. Dantus, Chem. Phys. 267 (2001) 99.
[13] B.I. Grimberg, V.V. Lozovoy, M. Dantus, S. Mukamel, J. Phys. Chem. 106 (2001).
[14] V.V. Lozovoy, I. Pastirk, E.J. Brown, B.I. Grimberg, M. Dantus, Int. Rev. Phys. Chem. 19 (2000) 531.
[15] I. Pastirk, V.V. Lozovoy, M. Dantus, Chem. Phys. Lett. 333 (2001) 76.
[16] T. Chen, V. Engel, M. Heid, W. Kiefer, G. Knopp, A. Materny, S. Meyer, R. Pausch, M. Schmitt, H. Schwoerer, T. Siebert, J. Mol. Struct. 481 (1999) 33.
[17] R. Zadoyan, V.A. Apkarian, Chem. Phys. Lett. 326 (2000) 1.
[18] G. Knopp, I. Pinkas, Y. Prior, J. Raman Spectrosc. 31 (2000) 51.
[19] R. Zadoyan, D. Kohen, D.A. Lidar, V.A. Apkarian, Chem. Phys. 266 (2001) 323.
[20] J. Tellinghuisen, J. Quant. Radiat. Transfer 19 (1978) 149.
[21] T. Wilhel, E. Riedle, Opt. Lett. 22 (1997) 1494.
[22] A. Shirakawa, I. Sakane, M. Takasaka, T. Kobayashi, Appl. Phys. Lett. 74 (1999) 2268.
[23] A.M. Weiner, Rev. Sci. Instrum. 71 (2000) 1929.
[24] D.W. Schumacher, J.H. Hoogenraad, D. Pinkos, P.H. Bucksbaum, Phys. Rev. A. 52 (1995) 4719.
[25] R. Uberna, Z.A. Amitay, R.A. Loomis, S.R. Leone, Faraday Discuss. 113 (1999) 385.
[26] T. Hornung, R. Meier, R. de Vivie-Riedle, M. Motzkus, Chem. Phys. 267 (2001) 261.
[27] S. Gerstenkorn, P. Luc, J. Physique 46 (1985) 867.
[28] R. Jozsa, in: S. Huggett, L. Mason, K.P. Tod, S.T. Tsou, N.M.J. Woodhouse (Eds.), Geometric Issues in the Foundations of Science, Oxford University Press, Oxford, 1997.
[29] C.H. Bennett, D.P. DiVincenzo, Nature 404 (2000) 247.
[30] M. Ban, J. Mod. Opt. 45 (1998) 2315.
[31] J.A. Jones, Prog. Nucl. Magn. Reson. Spectrosc. 38 (2001) 325.
[32] W.S. Warren, Science 277 (1997) 1689.
[33] N. Linden, S. Popescu, Phys. Rev. Lett. 87 (2001) 047901.
[34] H.K. Cummins, J.A. Jones, Contemp. Phys. 41 (2000) 383.
[35] S. Lloyd, Phys. Rev. A 61 (2000) 010301.